Aircraft Trim Recovery from Highly Nonlinear Upset Conditions *

Bor-Chin Chang †, Harry G. Kwatny ‡, Elie R. Ballouz §, and David C. Hartman ¶
Drexel University, 3141, Chestnut Street, Philadelphia, PA, 19104.

Aircraft loss of control (LOC) can result from a large spectrum of causal and contributing factors and is manifested as flight outside of the normal operating envelope and not predictably altered by pilot (or flight system) control inputs. LOC can also be characterized by nonlinear aircraft effects that degrade handling (or flying) qualities, including kinematic and/or inertial coupling, disproportionately large responses to small state variable changes, and oscillatory and/or divergent behavior. Some specific examples of nonlinear upset phenomena include stall / spin, falling leaf, and roll-pitch coupling oscillations. Although LOC need not be unrecoverable, it will become so if proper action is not taken. Recovery depends upon the timely execution of two critical actions: 1.) Determination of a desired feasible trim condition that the aircraft is able to recover to and reside on; and 2.) Determination of a control strategy that is capable of bringing the aircraft back to fly at the desired trim condition. This paper will investigate aircraft recovery from highly nonlinear upset conditions to a desired stable trim point that can be safely maintained. The test bed is a 6 d.o.f 12-state flight dynamics simulation model of an FA-18 like aircraft, which is nonlinear, flight-condition dependent. The proposed LOC prevention and recovery control strategies may also be applied to transport aircraft configurations for which nonlinear upset data is available.

Nomenclature

LOC	Loss of Control (in-flight)
$NASA$	National Aeronautics and Space Administration
$NTSB$	National Transportation Safety Board
x	$\begin{bmatrix} V & \beta & \alpha & p & q & r & \phi & \theta & \psi & pN & pE & h \end{bmatrix}^T$ state vector of the 12-state F/A-18 full nonlinear flight dynamics model
u	$\begin{bmatrix} \delta_a & \delta_r & \delta_e & \delta_T \end{bmatrix}^T$ control input vector of the 12-state F/A-18 full nonlinear flight dynamics model
V	total speed (ft/s)
β	side slip (rad for computation, deg for display)
α	angle of attack (rad for computation, deg for display)
p	roll rate (rad/s for computation, deg/s for display)
q	pitch rate (rad/s for computation, deg/s for display)
r	yaw rate (rad/s for computation, deg/s for display)
ϕ	roll angle (rad for computation, deg for display)
θ	pitch angle (rad for computation, deg for display)
ψ	yaw angle (rad for computation, deg for display)
pN	position North (ft)
pE	position East (ft)

*This work was supported in part by Army Research Laboratory under contract W911NF-15-2-0042.
†Professor, AIAA Member
‡S. Herbert Raynes Professor
§Research Associate
¶Graduate Student

h	altitude (ft)
δ_T	thrust control (lb)
δ_e	elevator control (rad for computation, deg for display)
δ_a	ailron control (rad for computation, deg for display)
δ_r	rudder control (rad for computation, deg for display)

I. Introduction

In the past two decades, more than half of the fatal airliner aircraft accidents are caused by loss-of-control (LOC) in flight.[1] Aircraft LOC[2,3] is an abnormal flight condition that includes stall, unusual attitude, large pitch and roll motion, and lateral/longitudinal oscillations, etc., which may pose safety threat to the aircraft if no immediate action is taken to address it. A more detailed definition on aircraft LOC is discussed in Wilborn and Foster.[4] Most in-flight LOC accidents are triggered by precursor events including subsystem/component failures, external hazards, and human errors. Prevention measures can be employed to enhance subsystem/component maintenance, to select flight route that avoids hazardous regions, and to care for the flight crews making sure that human mistakes are minimized. In addition to the above ongoing prevention effort, a new-generation intelligent flight control system can and should be designed to automatically neutralize the effect of the LOC precursor events, to prevent the aircraft from entering LOC, and to perform LOC recovery in case the aircraft is already in an LOC condition.

For the intelligent flight control system mentioned above to become a reality, two thrusts of research areas are required. They are aircraft flight dynamics and control theory. The flight dynamics and behavior of the aircraft near or in the LOC regime[5] are very different from those inside the normal flight envelope, and are not well understood. Aircraft LOC recovery is an extremely challenging and formidable task for the pilots. The reaction time for LOC recovery usually is very limited, and the pilots need to act quickly, correctly, and avoid deepening the crisis. Under these emergency and critical situations, pilots certainly need help from the flight computer/control system to provide the sensing information of all relevant parameters, to detect and accommodate the faults, to warn or disallow human errors, and to perform LOC recovery via automated controller reconfiguration or adaptation.

In this paper, an F/A-18 12-state full nonlinear flight dynamics model is employed as a test bed to investigate the flight dynamics and control effects under LOC hazards to gain insights into effective recovery mechanisms. The reminder of this paper is organized as follows. A quick introduction of the 12-state untrimmed, nonlinear flight dynamics simulation model and a brief review of the fundamental system theory relevant to aircraft flight dynamics and control such as equilibrium, trim, stability, linearization, and region of attraction are given in Section II, the preliminary section. In Section III, three simple control actions were employed in the study of LOC prevention and recovery. The first one is a simple open-loop fixed manual control, the second one is an LQR state feedback controller, and the third one is a modified LQR controller which is able to handle large roll angle excursions. All three control actions are meant to keep the aircraft at a desired trim or recover the aircraft from an LOC condition to the desired trim. In Section IV, we firstly will design a nominal controller to perform altitude control via flight path tracking, and then investigate the issues arising from elevator jam failures and design a single fixed controller to accommodate arbitrary elevator jam positions. A brief discussion of the investigation results and conclusion will be given in Section V.

II. Preliminaries

A. Aircraft Flight Dynamics Model

The F/A-18 flight dynamics simulation model employed in the study was originally created by Buttrill et. al.[6] based on the wind tunnel data. The model, originally written in FORTRAN, was later converted into MATLAB function files by Chakraborty et. al.[7,8] This 9-state full nonlinear model was then employed to derive reduced linear and nonlinear trimmed models for controller design and simulations in their study in region of attraction (ROA).

For the reason of simplicity and flexibility, we converted the 9-state full nonlinear F/A-18 flight dynamics model in MATLAB function files into Simulink model files. Three navigation equations associated with the

three state variables: two for translational position and one for altitude, are added to the model to make it a 12-state full nonlinear flight dynamics model. This full model is employed in analysis, design, and simulations throughout all the work presented in the paper.

The 12-state full nonlinear model and the associated state variables and control inputs of the F/A-18 aircraft flight dynamics are described in the following. The model is represented by the state equation,

$$\dot{x}(t) = f\left(x(t), u(t)\right) \tag{1a}$$

where the state vector is

$$x = \begin{bmatrix} V & \beta & \alpha & p & q & r & \phi & \theta & \psi & pN & pE & h \end{bmatrix}^T \tag{1b}$$

and the control input is

$$u = \begin{bmatrix} \delta_a & \delta_r & \delta_e & \delta_T \end{bmatrix}^T \tag{1c}$$

The 12 state variables are

V: total speed (ft/s),	β: side slip (rad),	α: angle of attack (rad),
p: roll rate (rad/s),	q: pitch rate (rad/s),	r: yaw rate (rad/s),
ϕ : roll angle (rad),	θ: pitch angle (rad),	ψ: yaw angle (rad),
pN: position North (ft),	pE: position East (ft),	h: altitude (ft)

and the 4 control inputs are

δ_a: aileron (rad), δ_r: rudder, (rad) δ_e: elevator (rad), δ_T: thrust, (lb).

The equations of motion inside the state equation Eq. (1) are given as follows,

$$\dot{V} = -\frac{1}{m}\bar{q}SC_{Dw} + g(\cos\phi\cos\theta\sin\alpha\cos\beta + \sin\phi\cos\theta\sin\beta - \sin\theta\cos\alpha\cos\beta) + \frac{T}{m}\cos\alpha\cos\beta \tag{2a}$$

$$\dot{\beta} = -\frac{1}{mV}\bar{q}SC_{Yw} + p\sin\alpha - r\cos\alpha + \frac{g}{V}\cos\theta\sin\phi\cos\beta + \frac{\sin\beta}{V}\left(g\cos\alpha\sin\theta - g\sin\alpha\cos\phi\cos\theta + \frac{T}{m}\cos\alpha\right) \tag{2b}$$

$$\dot{\alpha} = -\frac{1}{mV\cos\beta}Lift + q - \tan\beta(p\cos\alpha + r\sin\alpha) + \frac{g}{V\cos\beta}\left(\cos\phi\cos\theta\cos\alpha + \sin\alpha\sin\theta\right) - \frac{T\sin\alpha}{mV\cos\beta} \tag{2c}$$

$$\dot{p} = ((I_{zz}L + I_{xz}N - (I_{xz}(I_{yy} - I_{xx} - I_{zz})p + (I_{xz}^2 + I_{zz}(I_{zz} - I_{yy}))r)q)/(I_{xx}I_{zz} - I_{xz}^2)) \tag{2d}$$

$$\dot{q} = ((M + (I_{zz} - I_{xx})pr + (r^2 - p^2)I_{xz}/I_{yy} \tag{2e}$$

$$\dot{r} = ((I_{xz}L + I_{xx}N + (I_{xz}(I_{yy} - I_{xx} - I_{zz})r + (I_{xz}^2 + I_{xx}(I_{xx} - I_{yy}))p)q)/(I_{xx}I_{zz} - I_{xz}^2)) \tag{2f}$$

$$\dot{\phi} = p + (q\sin(\phi) + r\cos(\phi))\tan(\theta) \tag{2g}$$

$$\dot{\theta} = q\cos(\phi) - r\sin(\phi) \tag{2h}$$

$$\dot{\psi} = (q\sin(\phi) + r\cos(\phi))\sec(\theta) \tag{2i}$$

$$\begin{aligned}\dot{p}_N = {} & \cos(\theta)\cos(\psi)V\cos(\beta)\cos(\alpha) + (\sin(\phi)\sin(\theta)\cos(\psi) - \cos(\phi)\sin(\psi))V\sin(\beta) \\ & + (\cos(\phi)\sin(\theta)\cos(\psi) + \sin(\phi)\sin(\psi))V\cos(\beta)\sin(\alpha)\end{aligned} \tag{2j}$$

$$\begin{aligned}\dot{p}_E = {} & \cos(\theta)\sin(\psi)V\cos(\beta)\cos(\alpha) + (\sin(\phi)\sin(\theta)\sin(\psi) + \cos(\phi)\cos(\psi))V\sin(\beta) \\ & + (\cos(\phi)\sin(\theta)\sin(\psi) - \sin(\phi)\cos(\psi))V\cos(\beta)\sin(\alpha)\end{aligned} \tag{2k}$$

$$\dot{h} = \sin(\theta)V\cos(\beta)\cos(\alpha) - \sin(\phi)\cos(\theta)V\sin(\beta) - \cos(\phi)\cos(\theta)V\cos(\beta)\sin(\alpha) \tag{2l}$$

The moment and force equations, the aerodynamic coefficients, and the aircraft physical parameters required in the above equations of motion can be found in Chakraborty et. al.[7,8]

B. Equilibrium, Trim, Linearization, and Region of Attraction

Equilibium, linearization, and region of attraction are common terms in systems theory; however, these terms may become confusing in aircraft flight dynamics especially when *trim*[9,10] is roughly considered as a synonym of *equilibrium*. Strictly speaking, a system is said to be at equilibrium if all its state variables are constant at steady state. However, four of the twelve state variables in Eq.(1b) are irrelevant to the aircraft stability analysis and LOC study. These four state variables are the two position variables, pN and pE, the altitude h, and the yaw angle, ψ. Therefore, the aircraft is said to be at equilibrium if the other eight state variables in Eq.(1b): the total speed V, side slip β, angle of attack α, roll rate p, pitch rate q, yaw rate r, roll angle ϕ , and pitch angle θ, are constant at steady state. An equilibrium can be stable or unstable; for example, the pendulum system has two equilibrium points: one is stable when the stick is at the straight downward position, and the other is unstable when the stick is at the straight upward position. A stable equilibrium means that any perturbed state due to disturbances or other reasons will be brought back to the equilibrium at steady state if the perturbed state is inside the region of attraction.

Usually an aircraft trim is meant to be a stable and desirable flight condition;[9,10] however, in some distressed situation especially when partial control authority is lost the aircraft has to fly at a desirable equilibrium that may be inherently unstable. Under the scenario that the elevator control surface is jammed and only the thrust control is available for longitudinal motion, there might be only one or even no equilibrium available for level flight to keep the aircraft afloat. If it does, it may be unstable depending on the jammed position. Unstable equilibrium is not an issue since it can be stabilized via feedback control as long as the impaired aircraft is still stabilizable.[11,12] On the other hand, a stable equilibrium can be undesirable, and an aircraft flying at or toward an undesired stable equilibrium may cause LOC problems or even crash.

A general practice of control system design is to select a desired equilibrium (trim), and design a linear or nonlinear controller so that the closed-loop system has desired performance at and around the equilibrium. Region of attraction (ROA) basically defines the applicable operating range of the system in the state space. The concept of ROA is important especially in the decision process of determining whether to engage a feedback controller or not in an LOC situation since an engagement of a control at the time when the state of the system is outside the ROA can deepen the crisis.

The aircraft flight dynamics model used in the simulations of this paper is untrimmed, nonlinear, and parameter dependent. Just like any other physical system, aircraft needs to fly at or around one equilibrium at a time. For each trim of interest, a specific linear or nonlinear controller can be designed to achieve the desired performance within the operating range (inside the region of attraction). Although a nonlinear controller may cover a wider operating range than its linear counterpart, a linear controller can cover a reasonable wide operating range and deliver excellent performance if it is adequately designed. In this paper, the fundamental linear optimal regulation and tracking control approaches[12–15] are employed to demonstrate the effectiveness of linear state-space controllers on the LOC prevention and recovery.

III. Recovery from an LOC Condition to a Stable Level Flight

As described in Section IIA, the aircraft dynamics is described by a set of first-order differential equations with 12 state variables and 4 control inputs,

$$\begin{aligned} x &= \begin{bmatrix} V & \beta & \alpha & p & q & r & \phi & \theta & \psi & pN & pE & h \end{bmatrix}^T \\ u &= \begin{bmatrix} \delta_a & \delta_r & \delta_e & \delta_T \end{bmatrix}^T \end{aligned} \tag{3}$$

Just like the solution of any differential equation, the aircraft behavior represented by the state vector $x(t)$ is determined by the initial state vector $x(0)$ and the control input vector $u(t)$. The effect of all the previous disturbances, turbulence, and control actions up to $t = 0$ is summarized and stored in the initial state vector that will continue to influence the flight of the aircraft after $t = 0$. It is still a challenge in finding formal ways to verify and validate the LOC prevention and recovery capability of an aircraft flight system. One tentative way of examining the LOC prevention capability is to disturb the state of the system away from its trim in a simulation (or virtual flight test), and observe if the system is able to converge back to the trim without entering an LOC. Similar procedure can also be performed to examine the LOC recovery capability of the system by engaging a recovery controller to rescue a system already in LOC. The testing initial state vector to be used in the simulations throughout the paper is similar to the one used by Chakraborty et. al.[7]

to create an LOC situation. This initial state vector is called Init F and denoted by x_0^F, a ferocious initial state vector, which represents the effect of the previous disturbances or erroneous control actions, is given by

$$Init\ F: x_0^F = \left[\begin{array}{cccccccccccc} 350\text{ft/s} & 20^\circ & 40^\circ & 10^\circ/\text{s} & 0 & 5^\circ/\text{s} & 0^\circ & 0^\circ & 0^\circ & 0\text{ft} & 0\text{ft} & 25000\text{ft} \end{array}\right] \tag{4}$$

Note that the initial state vector x_0^F foretells the coming of a very violent flight condition with the information: side slip 20°, angle of attack 40°, roll rate 10°/s, yaw rate 5°/s, and a steep descending flight path angle $\gamma = \theta - \alpha = 0^\circ - 40^\circ = -40^\circ$.

To present the design of the LOC recovery controller and show how the LOC recovery simulations are conducted, we will start from the simulation schematic diagram shown in Figure 1. The block in the right is the aircraft flight dynamics model, which is basically the same as described in Section IIA except the inputs are required to satisfy the constraints specified by the limiters and actuator dynamics shown in Figure 2. The state vector x of the untrimmed aircraft flight dynamics model is assumed available for feedback, but it needs to be subtracted by $Trim_x$ to become $\bar{x}$ to serve as the input to the controller. The output of the controller is $\bar{u}$, which needs to be added by $Trim_u$ to make u as the control input to the aircraft flight dynamics model via the Actuator Dynamics and Limiter block. $Trim_x$ and $Trim_u$ are the trimmed state and trimmed control input of the flight dynamics model, respectively. In other words, $Trim_x$ and $Trim_u$ together represent the selected operating trim (equilibrium), and the controller is designed specifically with respect to the trim and the operating range around it. In the $\bar{x}$-$\bar{u}$ coordinates, the origin represents the operating trim. When (x, u) is at the trim, ($\bar{x}$, $\bar{u}$) is at the origin.

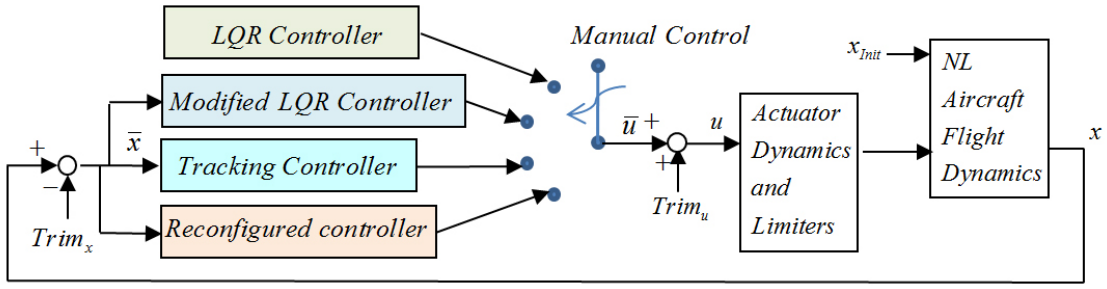

Figure 1. Schematic diagram for LOC recovery simulations using switching controls

	Saturation limits	Rate limits	Dynamics
Ailron δ_a	$-25^\circ < \delta_a < 25^\circ$	$-100^\circ/s < \dot{\delta}_a < 100^\circ/s$	$48/(s+48)$
Rudder δ_r	$-30^\circ < \delta_r < 30^\circ$	$-61^\circ/s < \dot{\delta}_r < 61^\circ/s$	$40/(s+40)$
Elevator δ_e	$-24^\circ < \delta_e < 10.5^\circ$	$-40^\circ/s < \dot{\delta}_e < 40^\circ/s$	$30/(s+30)$
Thrust δ_T	$0\text{ lb} < \delta_T < 20{,}000\text{ lb}$		$30/(s+30)$

Figure 2. Saturation and rate limits and actuator dynamics constraints

The Selection Switch on the right of the controllers in general can be controlled by an automatic switching logic or by the pilot based on flight mode changes or special situations. When a control switching is made, the trim may need to change accordingly. The four controllers shown in Figure 1 are all designed with respect to the same trim, which is a straight level flight with 10 degree of angle of attack. This particular trim is called Trim A that can be obtained as follows either by numerical search or simulation:

$$Trim\ A: \left\{\begin{array}{l} x_A = \left[\begin{array}{cccccccccccc} 435.9\text{ft/s} & 0^\circ & 10^\circ & 0^\circ/s & 0^\circ/s & 0^\circ/s & 0^\circ & 10^\circ & *^\circ & *\text{ft} & *\text{ft} & *\text{ft} \end{array}\right]^T \\ u_A = \left[\begin{array}{cccc} 0^\circ & 0^\circ & -1.26^\circ & 5470.5\text{lb} \end{array}\right] \end{array}\right. \tag{5}$$

In the rest of this section, we will consider three control actions regarding to the prevention and recovery of the LOC scenario caused by the ferocious initial state x_0^F given in Eq.(4). The first control action under test will be a fixed manual control at Trim A without the aid of any feedback control. Then a regular LQR feedback controller designed specifically for Trim A will be used in the second control action. The third one is a modified LQR controller in which the LQR controller is modified to address the issue caused by large roll excursions. The discussion of the other two controllers: Tracking controller and Reconfigured controller will be given in the next section.

A. A Fixed Manual Control at Trim A for LOC Prevention and Recovery

In this simulation, only a fixed manual control $u_A = \begin{bmatrix} 0^\circ & 0^\circ & -1.26^\circ & 5470.5\text{lb} \end{bmatrix}^T$ is applied to the input of the flight dynamics model without the aid of any feedback control. Figure 3 records part of the state response due to the initial state x_0^F, in which the left column shows the transient behavior and the right column clearly exhibits that the steady-state response. It can be seen from the left column of Figure 3 that

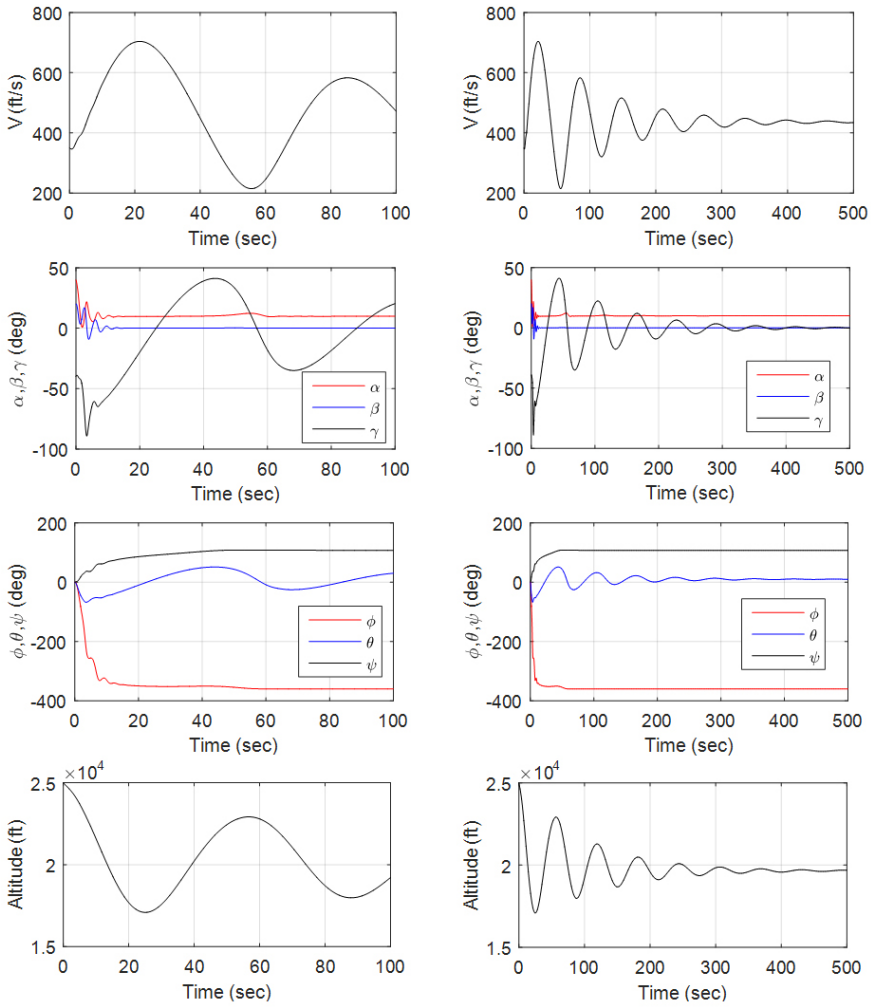

Figure 3. The response of the aircraft with fixed manual control at Trim A due to the initial state x_0^F

$x(0) = x_0^F$ at $t = 0$, and things happen rather quickly that within 3 seconds the aircraft has rolled to the left by more than 200° and pitched down to 80°, which certainly is a very difficult loss-of-control situation. Then the aircraft continued its wide ride: it rolls to about -360° position, which completes one full 360° roll excursion, and pitches up and down between -80° and $+60^\circ$ for a long period of time. The speed V and the altitude h also exhibit the up and down excursions with the same frequency. A few snap shots of the wide movements are shown in the left column of Figure 4.

Nevertheless, it does converge although slowly - after 500 seconds the aircraft recovers to a stable straight level flight with 10° angle of attack, which is exactly the Trim A condition as shown in the right column of Figure 3.

Figure 4. Snapshots of the aircraft flight with fixed manual control (left column) and with LQR feedback control (right column).

To explain why it can be possible to recover from an LOC to a stable level flight just by using a fixed open-loop manual control, we will examine the system property at the trim. For the trim of a straight level flight with 10° angle of attack, given in Eq.(5) as Trim A, a linearized state-space model with decoupled longitudinal and lateral dynamics state equations can be obtained via the standard Jacobian approach as follows,

$$
\begin{aligned}
&\dot{\bar{x}}_{Lg}(t) = A_{Lg}\bar{x}_{Lg}(t) + B_{Lg}\bar{u}_{Lg}(t) \\
&\bar{x}_{Lg} = \begin{bmatrix} \bar{V} & \bar{\alpha} & \bar{q} & \bar{\theta} \end{bmatrix}^T, \quad \bar{u}_{Lg} = \begin{bmatrix} \bar{\delta}_e & \bar{\delta}_T \end{bmatrix} \\
&A_{Lg} = \begin{bmatrix} -0.0239 & -28.3172 & 0 & -32.2 \\ -0.0003 & -0.3621 & 1 & 0 \\ 0 & -2.2115 & -0.2532 & 0 \\ 0 & 0 & 1 & 0 \end{bmatrix}, \quad B_{Lg} = \begin{bmatrix} -3.8114 & 0.001 \\ -0.0515 & 0 \\ -2.8791 & 0 \\ 0 & 0 \end{bmatrix}
\end{aligned} \tag{6}
$$

and

$$\dot{\bar{x}}_{La}(t) = A_{La}\bar{x}_{La}(t) + B_{La}\bar{u}_{La}(t)$$
$$\bar{x}_{La} = \begin{bmatrix} \bar{\beta} & \bar{p} & \bar{r} & \bar{\phi} \end{bmatrix}^T, \quad u_{La} = \begin{bmatrix} \bar{\delta}_a & \bar{\delta}_r \end{bmatrix}^T$$
$$A_{La} = \begin{bmatrix} -0.0347 & 0.1736 & -0.9848 & 0.0727 \\ -8.543 & -0.8883 & 0.8762 & 0 \\ 0.886 & 0.0399 & -0.1895 & 0 \\ 0 & 1 & 0.1763 & 0 \end{bmatrix}, \quad B_{La} = \begin{bmatrix} -0.0149 & 0.0207 \\ 8.3321 & 0.9541 \\ -0.042 & -0.6277 \\ 0 & 0 \end{bmatrix} \tag{7}$$

It can be found that the eigenvalues associated with the longitudinal dynamics are $-0.3094 \pm j1.4799$ and $-0.0101 \pm j0.1008$, and the eigenvalues for the lateral dynamics are $-0.2873 \pm j1.453$, -0.4888, and -0.0518. The trim is stable although the longitudinal dynamics has a very small damping ratio $\varsigma = 0.1$ and slow natural frequency $\omega_n = 0.101$rad/s. Note that the damping ratio and natural frequency match very well with the lightly damped and the long oscillation period in the longitudinal responses shown in Figure 3.

The trim is stable, and it appears that the state of the system falls into the region of attraction when the roll angle position is close to $-360°$. Strictly speaking, mathematically the equilibrium with ϕ at $-360°$ is not the original equilibrium at ϕ=$-360°$. However, physically these two angles are at the same angular position.

B. An LQR Feedback Control at Trim A for LOC Prevention and Recovery

For this simulation, the Controller Selection Switch in Figure 1 is set at the *LQR Controller* position, and the structure of the controller is shown in Figure 5, in which the two LQR controllers, F_{Lg} and F_{La} are specifically designed for the aircraft to operate at and around Trim A.

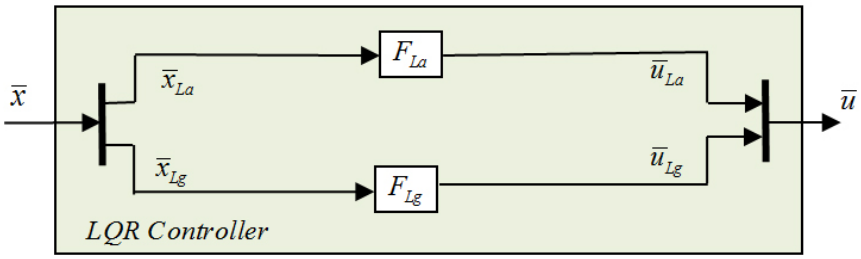

Figure 5. Structure of the LQR controller designed specifically for Trim A

Based on the longitudinal state equation in Eq.(6), an optimal longitudinal state feedback controller,

$$\bar{u}_{Lg}(t) = F_{Lg}\bar{x}_{Lg}$$
$$F_{Lg} = \begin{bmatrix} -0.0028 & -0.2725 & 0.1370 & 0.3315 \\ -0.0326 & -0.7685 & 0.9373 & 1.4266 \end{bmatrix} \tag{8}$$

is found to minimize the following performance index,

$$J_{Lg} = \int_0^\infty \left(x_{Lg}^T(t) Q_{Lg} x_{Lg}(t) + u_{Lg}^T(t) R_{Lg} u_{Lg}(t) \right) dt$$
$$\text{with } Q_{Lg} = diag\{0.01,\ 1,\ 1,\ 1\},\ R_{Lg} = diag\{1000,\ 0.001\} \tag{9}$$

Similarly, based on the lateral state equation in Eq.(7), an optimal lateral state feedback controller,

$$\bar{u}_{La}(t) = F_{La}\bar{x}_{La}$$
$$F_{La} = \begin{bmatrix} 0.8739 & -0.8937 & -0.3573 & -0.3094 \\ -1.8130 & -0.7223 & 2.6598 & -0.1995 \end{bmatrix} \tag{10}$$

is found to minimize the following performance index,

$$J_{La} = \int_0^\infty \left(x_{La}^T(t) Q_{La} x_{La}(t) + u_{La}^T(t) R_{La} u_{La}(t) \right) dt$$
$$\text{with } Q_{La} = diag\{10,\ 100,\ 10,\ 10\},\ R_{La} = diag\{100,\ 10\} \tag{11}$$

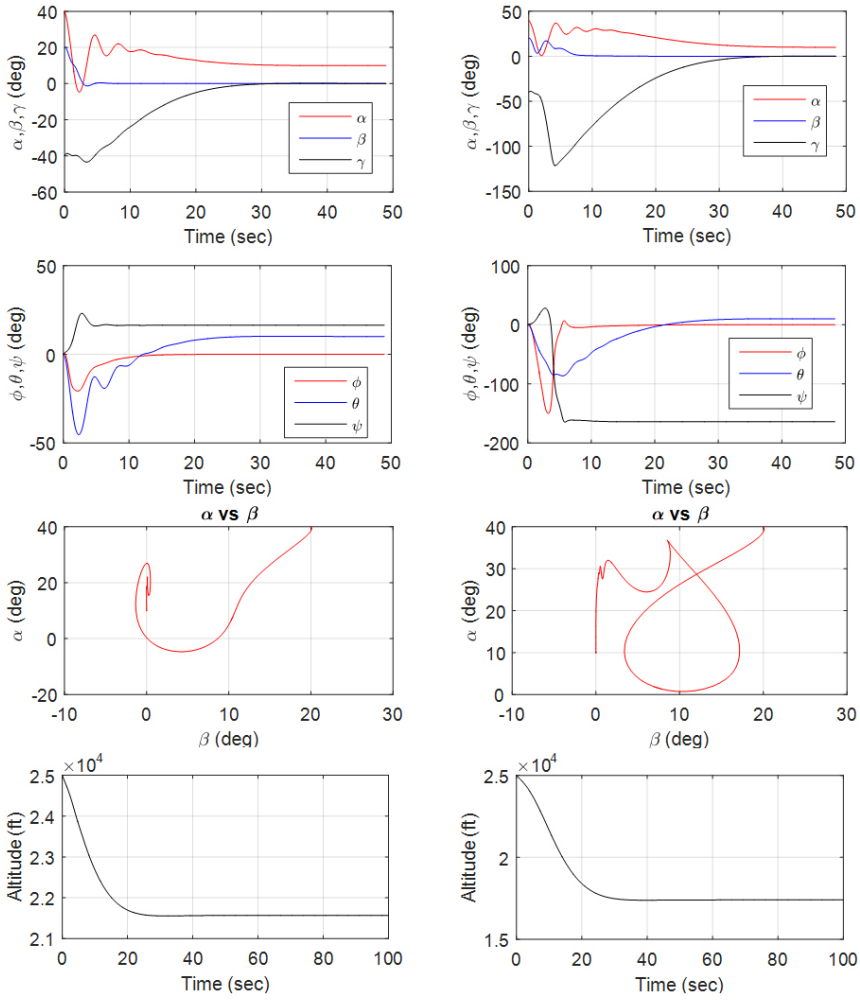

Figure 6. The response of the aircraft with LQR feedback control at Trim A due to the initial state x_0^F. Left column: LQR controller engaged at $t = 0$, Right column: LQR controller engaged at $t = 2.4s$.

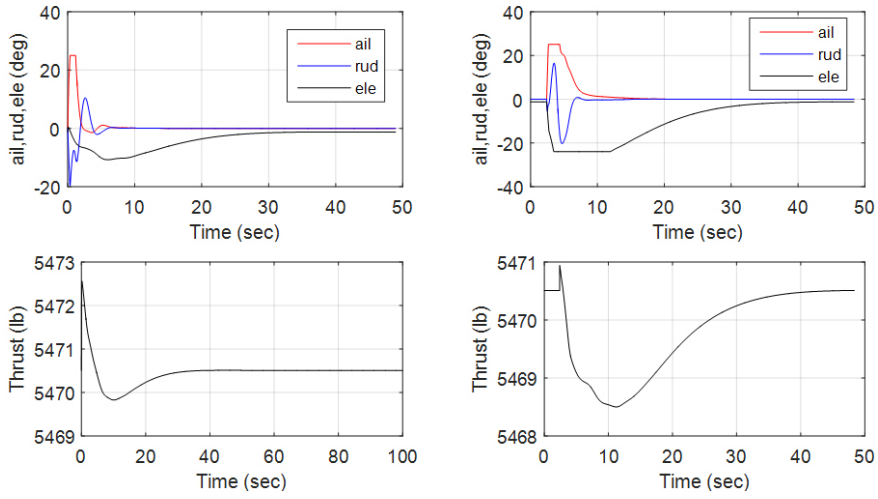

Figure 7. The control input of the aircraft with LQR feedback control at Trim A due to the initial state x_0^F. Left column: LQR controller engaged at $t = 0$, Right column: LQR controller engaged at $t = 2.4s$.

The left and right columns of Figure 6 and Figure 7 record the LOC responses of the system with LQR controllers engaged at $t = 0$ and $t = 2.4s$, respectively. When engaged at the very beginning, the controller is able to keep the roll and pitch angles under control to the desired 0° and 10°, respectively, and bring the closed-loop system to Trim A in less than 30 second. With a late engagement at $t = 2.4s$, the LQR controller is still able to recover the system from an LOC condition with $\phi = -150°$ and $\theta = -80°$ to the Trim A condition, a straight level flight with 10° angle of attack. It is clear that the performance of the LQR feedback control is better than that of the fixed manual control in terms of LOC prevention and LOC recovery. The comparison is also clearly illustrated in Figure 4 in which the snap shots and flight data of the LQR feedback control on the right column reveal much better LOC prevention and recovery performance than those of the fixed manual control on the left column.

The comparison of the two controls can also be interpreted according to pole (eigenvalue) locations. The switch from the manual control to the LQR feedback control has changed the longitudinal eigenvalues from $-0.3094 \pm j1.4799$, $-0.0101 \pm j0.1008$, which are the eigenvalues of A_{Lg}, to $-0.3344 \pm j1.4927$, $-0.1702 \pm j0.1126$, which are the eigenvalues of $A_{Lg} + B_{Lg}F_{Lg}$. Note that the damping ratio has changed from $\varsigma = 0.1$ to $\varsigma = 0.85$ and the natural frequency from $\omega_n = 0.101$rad/s to $0.2rad/s$. Meanwhile, the lateral eigenvalues have changed from $-0.2873 \pm j1.453$, -0.4888, -0.0518, which are the eigenvalues of A_{La}, to $-0.2873 \pm j1.453$, -0.4888, -0.0518, which are the eigenvalues of $A_{La} + B_{La}F_{La}$. Note that the increases of both damping ratio and natural frequency for both longitudinal and lateral dynamics have enhanced the stability and increased the rate of convergence to the desired equilibrium.

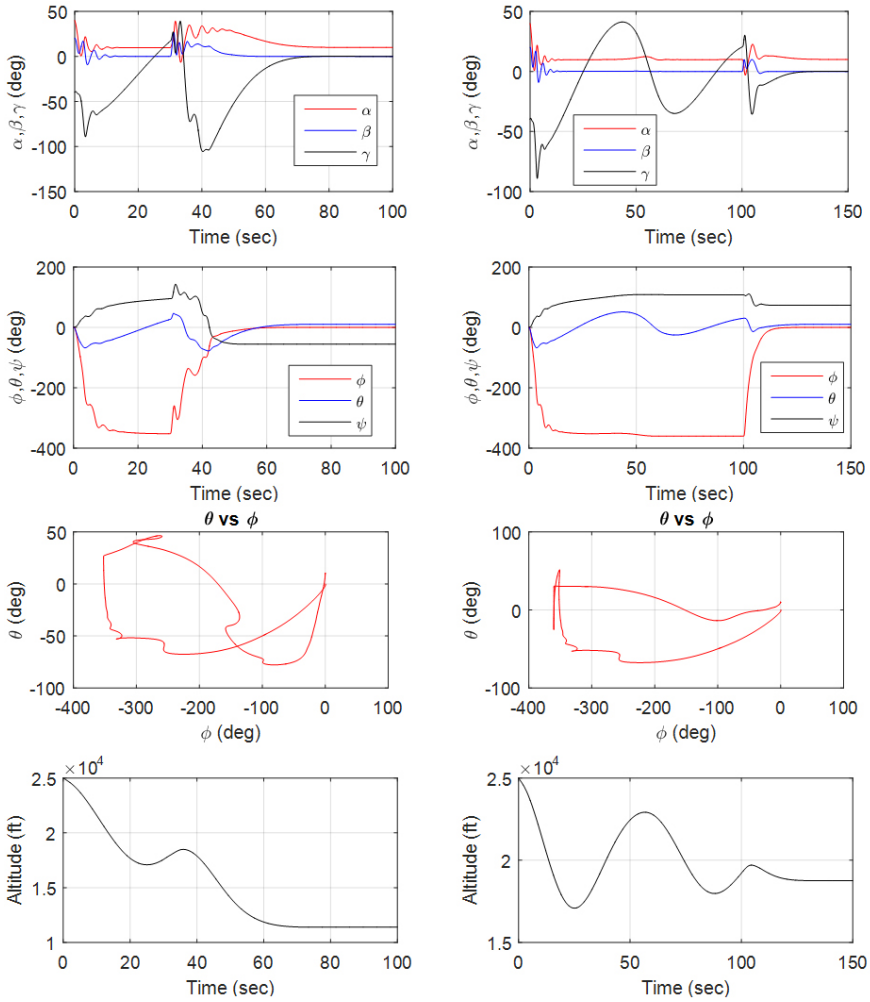

Figure 8. The response of the aircraft with the LQR feedback control. Left column: LQR controller engaged at $t = 30s$, Right column: LQR controller engaged at $t = 100s$.

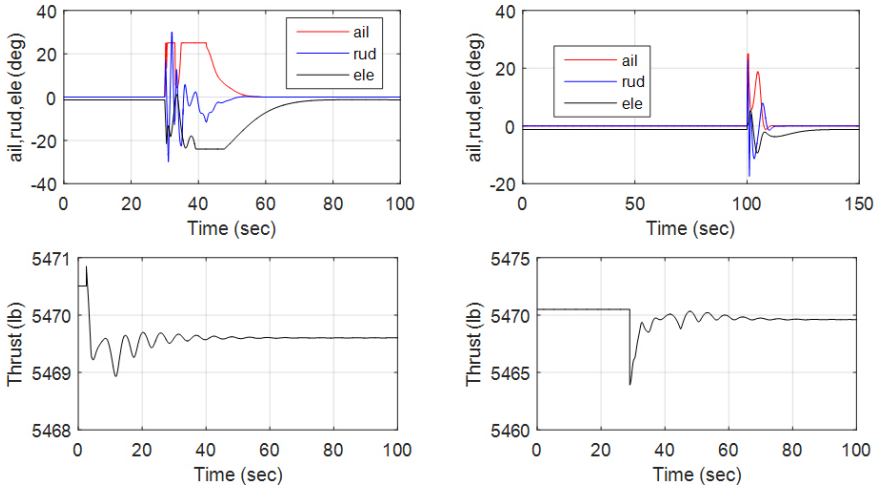

Figure 9. The control input of the aircraft with LQR feedback control. Left column: LQR controller engaged at $t = 30s$, Right column: LQR controller engaged at $t = 100s$.

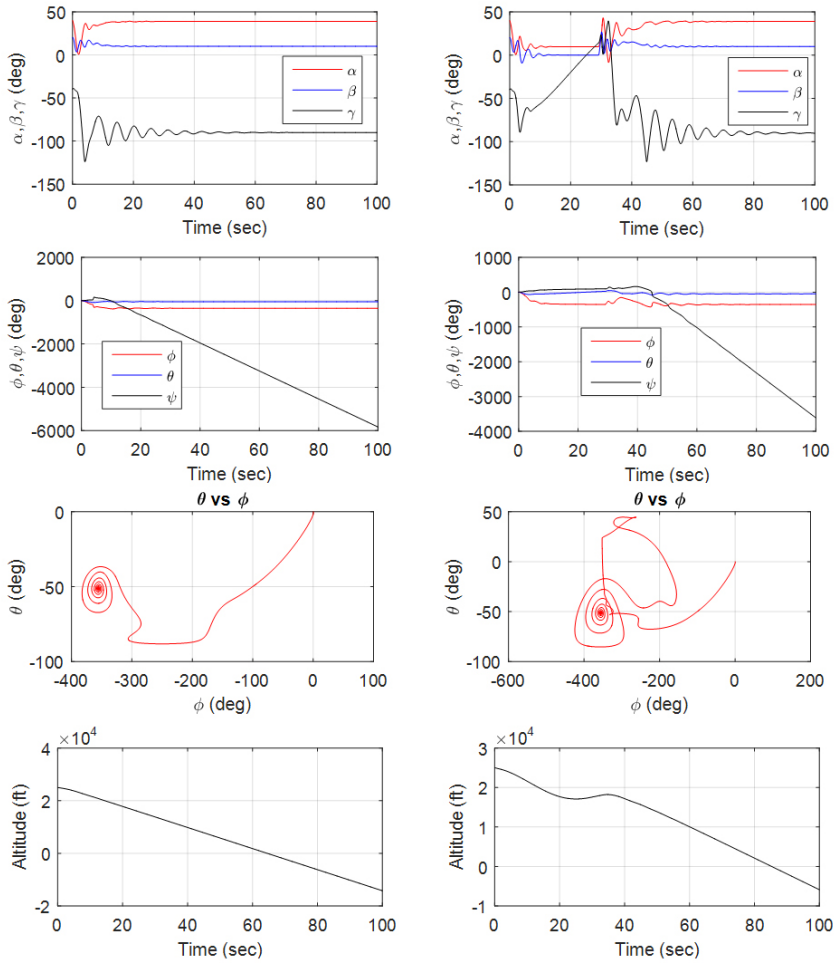

Figure 10. The response of the aircraft with the LQR feedback control. Left column: LQR controller engaged at $t = 2.5s$, Right column: LQR controller engaged at $t = 29s$.

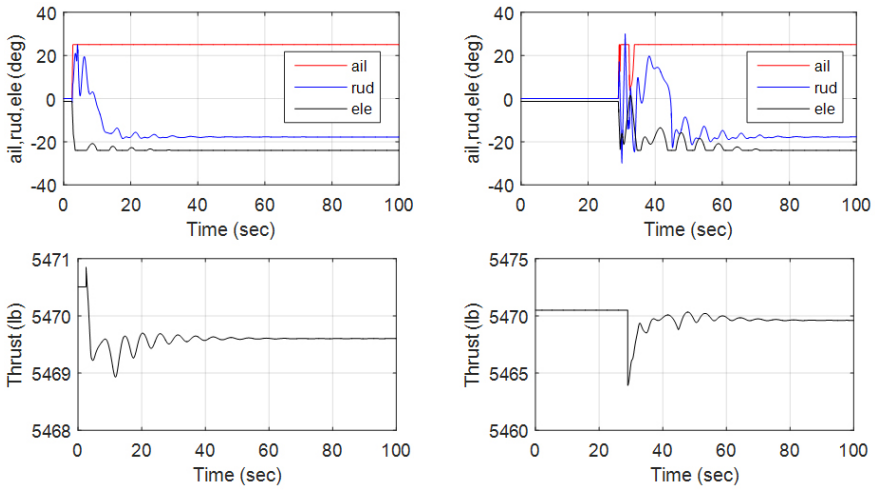

Figure 11. The control input of the aircraft with LQR feedback control. Left column: LQR controller engaged at $t = 2.5s$, Right column: LQR controller engaged at $t = 29s$.

The time of switching from the manual control (or a nominal controller) to the LQR control (or an LOC recovery controller) is critical. A switching made at a wrong time can deepen the LOC situation and make it even more difficult to recover. For the LOC case with the LQR controller considered in this subsection, the aircraft is recoverable to Trim A with roll angle $\phi = 0°$ during the early period from $t = 0$ to $t = 2.4s$. It is also recoverable to Trim A with zero roll angle at a later time after $t = 30s$ as shown in Figure 8 and Figure 9. However, if the LQR controller is engaged during the time between $t = 2.5s$ and $t = 29s$, the system will either become unstable or converge to an undesired equilibrium that may lead the aircraft to crash. As shown in Figure 10 and Figure 11, the LQR controller does not have enough control input resources to bring the system to the desired trim; instead, the system converges to an undesired equilibrium, Equilibrium X, as

$$Equil\ X: \begin{cases} x_X = \begin{bmatrix} 463\text{ft/s} & 10° & 39° & -50°/s & -3°/s & -40°/s & -355° & -51° & *° & *\text{ft} & *\text{ft} & *\text{ft} \end{bmatrix}^T \\ u_X = \begin{bmatrix} 25° & -17.8° & -24° & 5469.6\text{lb} \end{bmatrix} \end{cases} \tag{12}$$

Note that both of simulation results on the left and right columns in Figure 10 and Figure 11 (the controller engaged at $t = 2.5s$ or $t = 29s$) indicate that the aircraft will be attracted to the above undesired equilibrium, which has a flight path angle $\gamma = -90°$ that would crash the aircraft shortly after $t = 60s$ or $t = 80s$ as shown in the left and right columns, respectively, of Figure 10.

It is interesting to note that the aircraft is recoverable when the time is either before $t = 2.4s$ or after $t = 30s$. A reasonable explanation is that the system is inside the ROA (region of attraction) during these two time zones. In the early stage, the effect due to the initial state (or disturbances/erroneous control actions) is still not fully developed. On the other hand, the LOC effect will decay as time goes by if the trim set by the fixed manual control is stable. With a decrease of the LOC effect, the system may reenter the ROA so that the controller is able to bring the system to the desired trim.

An analysis of the failed recovery between $t = 2.5s$ and $t = 29s$ and a possible remedy of the failure will be discussed in the next subsection.

C. A Modified LQR Feedback Control at Trim A for LOC Prevention and Recovery

From the simulations in the previous subsection, Section IIIB, the aircraft will pitch down to about $-88°$ and roll to the left to more than $200°$ in less than 3 seconds if the LQR controller is not engaged successfully within 2.4 seconds. Furthermore, most of the LQR controller action engaged during the period between $t = 2.5s$ and $t = 29s$ will bring the system to the undesired equilibrium, Equil X, given by Eq.(12). By observing the control inputs at the equilibrium, the ailron control and elevator control are both at their saturation limits, $\delta_a = 25°$ and $\delta_e = -24°$. It appears that the LQR controller attempts to go against

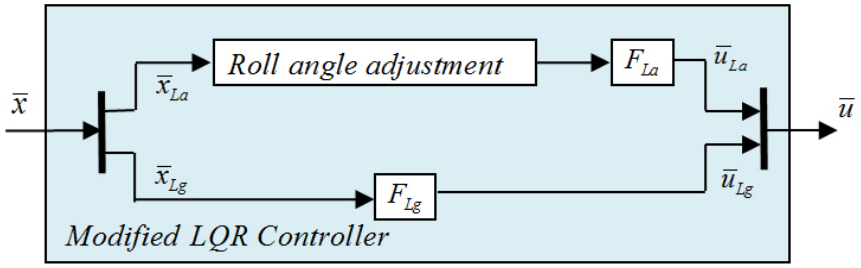

Figure 12. Structure of the Modified LQR controller designed specifically for Trim A

the tide to bring the roll angle back to $\phi = 0°$ instead of just letting it roll towards $\phi = -360°$. Although physically 0° and 360° mean exactly the same angular position, the LQR controller considers that the aircraft is 360° out of position if $\phi = -360°$. The controller needs to recognize that a $-300°$ angle actually is an angle of $+60°$, and to bring $+60°$ to 0° is much easier.

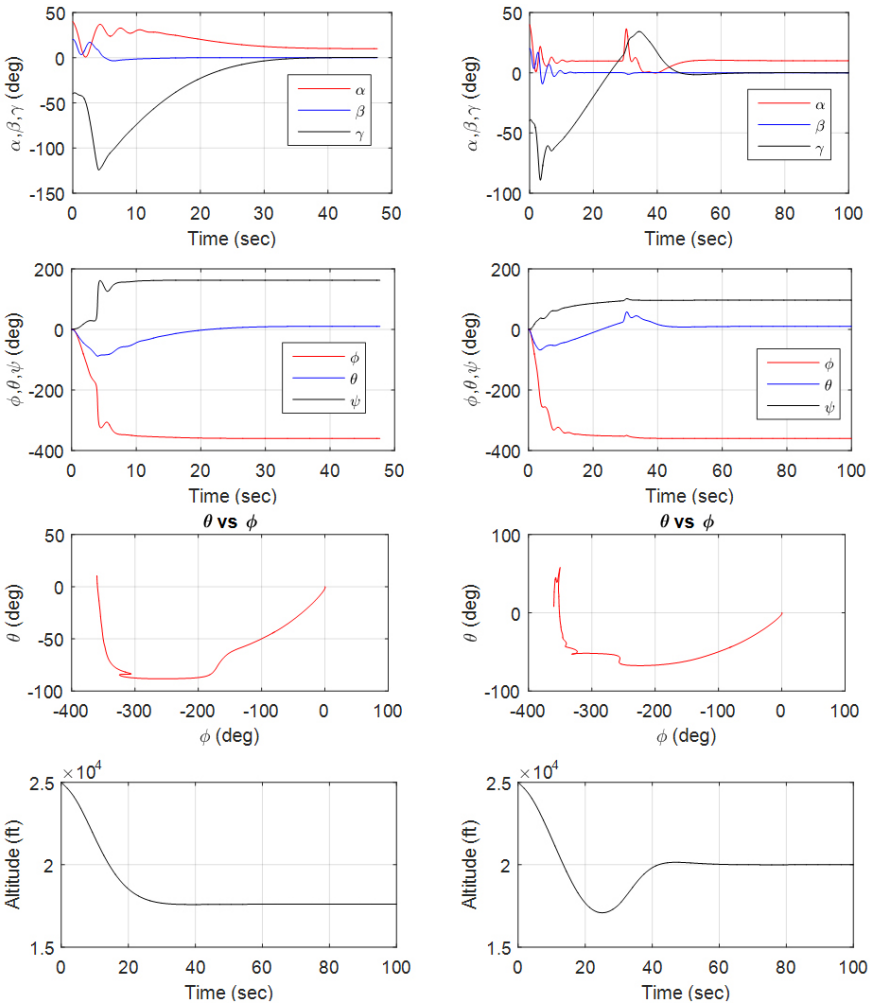

Figure 13. The response of the aircraft with the modified LQR feedback control. Left column: Modified LQR controller engaged at $t = 2.5s$, Right column: Modified LQR controller engaged at $t = 29s$.

To resolve this issue, a simple roll angle adjustment logic is added to the LQR controller to make it a modified LQR controller as shown in Figure 12. With the modified LQR controller, the LOC condition caused by the initial state, x_0^F given in Eq.(4), can be recovered to Trim A, a straight level flight with

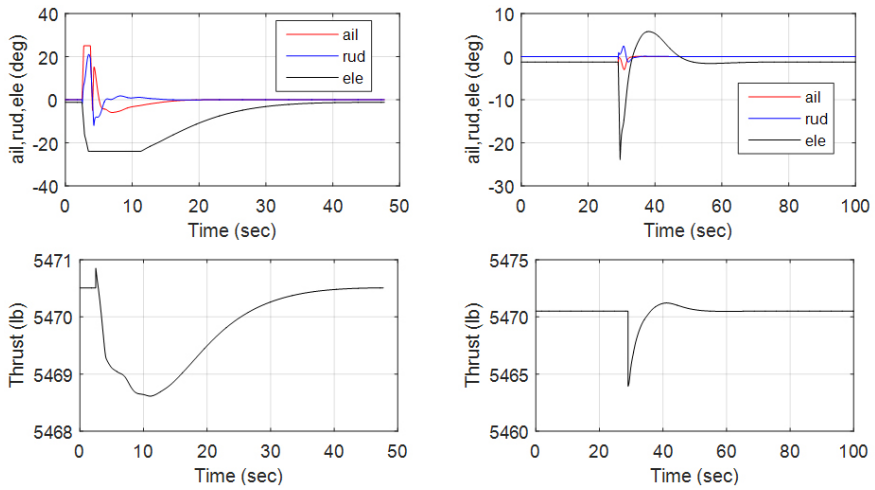

Figure 14. The control input of the aircraft with LQR feedback control. Left column: Modified LQR controller engaged at $t = 2.5s$, Right column: Modified LQR controller engaged at $t = 29s$.

10° angle of attack, despite the controller engagement time. As shown in Figure 13 and Figure 14, any engagement time between $t = 2.5s$ and $t = 29s$ is now recoverable to Trim A in less than 35 seconds.

IV. Tracking and Reconfigured Control for Elevator Jam Failure

This section will be divided into two subsections, one for altitude control via flight path tracking and another for the same problem under the elevator jam failure condition. The elevator jam position is assumed unknown *a priori*, but its position information will be available for feedback when it occurs. Furthermore the tracking controller will be a fixed controller capable of neutralizing the disturbances created by a range of elevator jam positions.

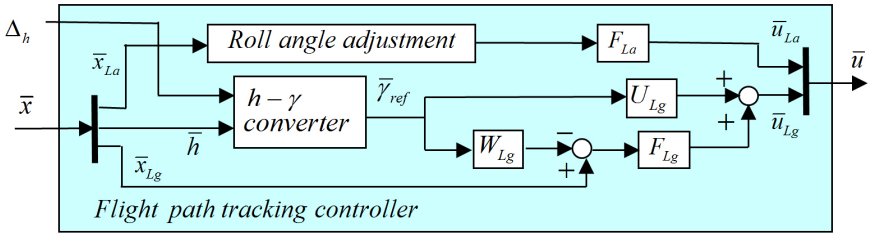

Figure 15. Structure of the flight path tracking controller designed specifically for Trim A

A. Altitude Control via Flight Path Tracking

The structure of the flight path tracking controller designed specifically for Trim A is shown in Figure 15. The matrices F_{La} and F_{Lg} designed in Section III will continue to be used in this subsection. The tracking regulator matrices W_{Lg} and U_{Lg} can be obtained as

$$\begin{aligned} W_{Lg} &= \begin{bmatrix} 435 & -0.463913 & 0 & 0.536087 \end{bmatrix}^T \\ U_{Lg} &= \begin{bmatrix} 0.356339 & 16677.9 \end{bmatrix}^T \end{aligned} \tag{13}$$

by solving the following equations,

$$\begin{aligned} A_{Lg}W_{Lg} + B_{Lg}U_{Lg} &= 0 \\ C_{1u}W_{Lg} + D_{11u}U_{Lg} &= 0 \end{aligned} \tag{14}$$

with $C_{1u} = \begin{bmatrix} 0 & 1 & 0 & -1 \end{bmatrix}$ and $D_{11u} = 1$ chosen for flight path tracking.

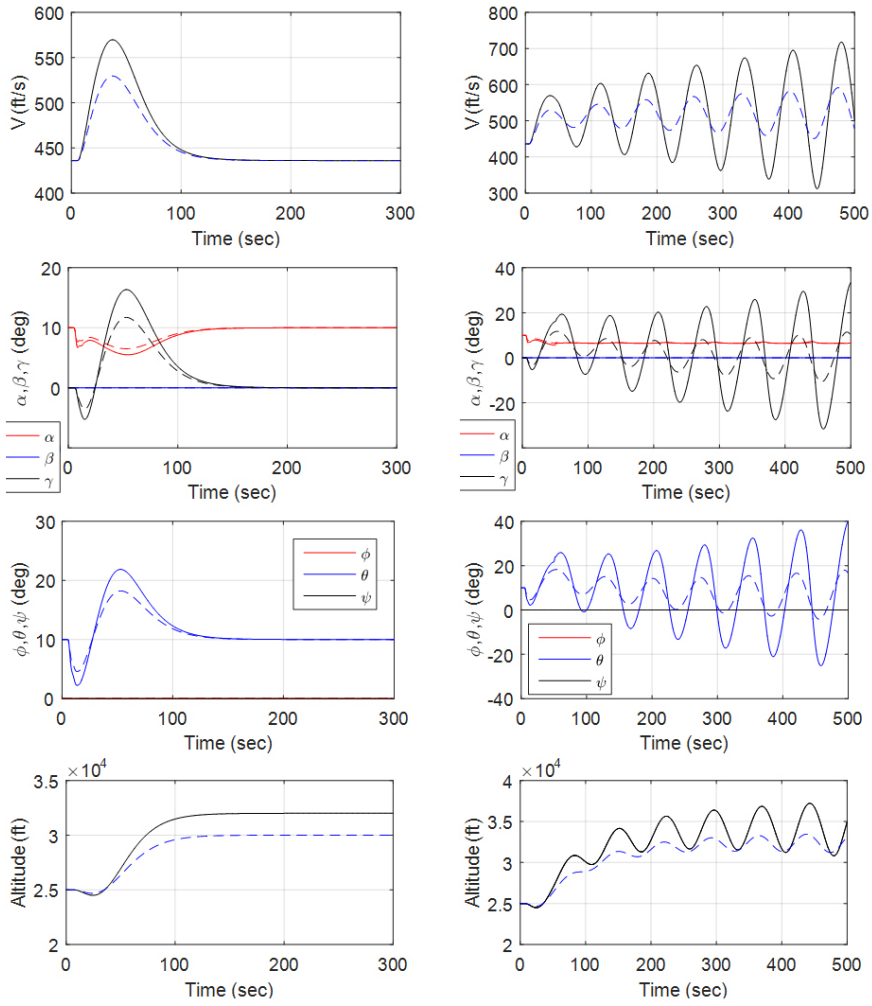

Figure 16. The response of the aircraft with altitude control via flight path tracking. Left column: Nominal altitude control responses - 7000ft ascent (solid line) and 5000ft ascent (dashed line), Right column: Unstable responses due to the elevator jam at 1.28° occurred $t = 50s$.

The $h - \gamma$ Converter block is employed to determine the desired flight path angle γ according to the altitude control differential Δ_h and the actual altitude output. With the flight path tracking controller, the altitude of the aircraft can be smoothly controlled as shown in the left column Figure 16 and Figure 17. The aircraft is assumed conducting a straight level flight with 10° angle of attack (Trim A) initially, and the 7000ft (or 5000ft) ascent maneuver starts at $t = 5s$. It can be seen from the graphs on the left column of Figure 17 and Figure 16 that both the elevator δ_e and the thrust δ_T work together to control the flight path to achieve the desired altitude ascent and resume to the trim at the new altitude. The fixed tracking controller is capable of handling a range of ascent and descent.

The graphs on the right column of Figure 16 and Figure 17 demonstrate how an elevator jam failure would affect the stability and performance of the system. Assume the aircraft in the beginning is conducting the same 7000ft (or 5000ft) accent maneuver using the same tracking controller, but at $t = 50s$ the elevator is jammed at the 1.28° position. The elevator jam failure not only causes a loss of control authority, it also creates a persistent disturbance against the flight of the aircraft. If no action is taken to address the failure issue and the nominal tracking controller is still in action, the tracking performance would be poor and the system might become unstable as indicated by the time response graphs on the right column of Figure 16 and Figure 17.

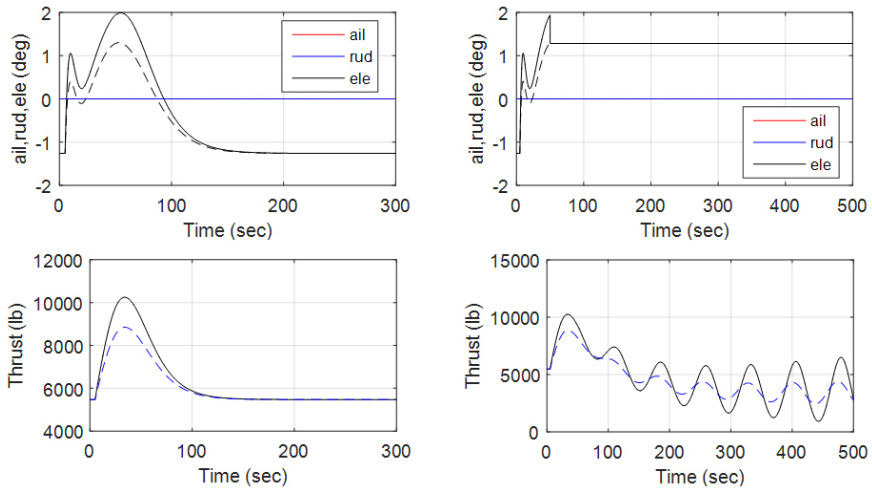

Figure 17. The control input of the aircraft with altitude control via flight path tracking. Left column: Nominal altitude control responses - 7000ft ascent (solid line) and 5000ft ascent (dashed line), Right column: Unstable responses due to the elevator jam at 1.28° occurred $t = 50s$.

B. Controller Reconfiguration to Accommodate the Elevator Jam Failure

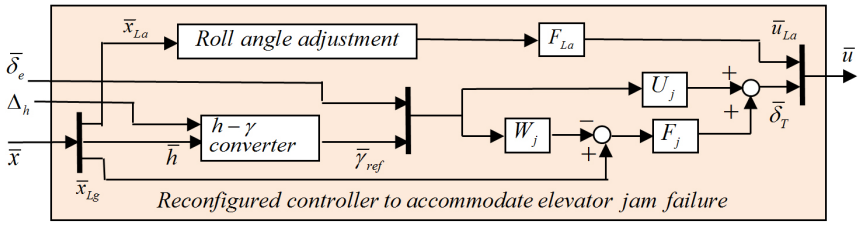

Figure 18. Structure of the reconfigured controller to accommodate the elevator jam failure

The structure of the reconfigured flight path tracking controller designed to accommodate the elevator jam failure is shown in Figure 18. The lateral LQR controller F_{La} will remain the same, but the longitudinal controller is required to be designed to address the elevator jam and flight path tracking according to the new longitudinal state equation,

$$\dot{\bar{x}}_{Lg}(t) = A_{Lg}\bar{x}_{Lg}(t) + B_j\bar{\delta}_T(t) + \begin{bmatrix} B_e & 0 \end{bmatrix}\begin{bmatrix} \bar{\delta}_e \\ \bar{\gamma}_{ref} \end{bmatrix} \tag{15}$$

where $\begin{bmatrix} B_e & B_j \end{bmatrix} = B_{Lg}$ and $\bar{\delta}_e$ becomes a persistent disturbance, not a control input anymore. F_j is designed as

$$F_j = \begin{bmatrix} -81.2 & 4345.6 & 1417.4 & -3345 \end{bmatrix} \tag{16}$$

via the optimal solution that minimizes the following performance index,

$$\begin{aligned} &J_j = \int_0^\infty \left(x_{Lg}^T(t)Q_j x_{Lg}(t) + \delta_T^T(t)R_j\delta_T(t)\right)dt \\ &\text{with } Q_j = diag\{1,\ 1,\ 1,\ 1\},\ R_j = 0.0001 \end{aligned} \tag{17}$$

With the above F_j, the longitudinal closed-loop poles will be at $-0.3095 \pm j1.4799, \quad -0.0496 \pm j0.0887$.

The tracking regulator matrices W_j and U_j can be obtained as

$$W_j = \begin{bmatrix} 1328.6 & -38.4324 \\ -1.30189 & 0 \\ 0 & 0 \\ -1.30189 & 1 \end{bmatrix}, \quad U_j = \begin{bmatrix} -45412.5 & 32860.2 \end{bmatrix} \tag{18}$$

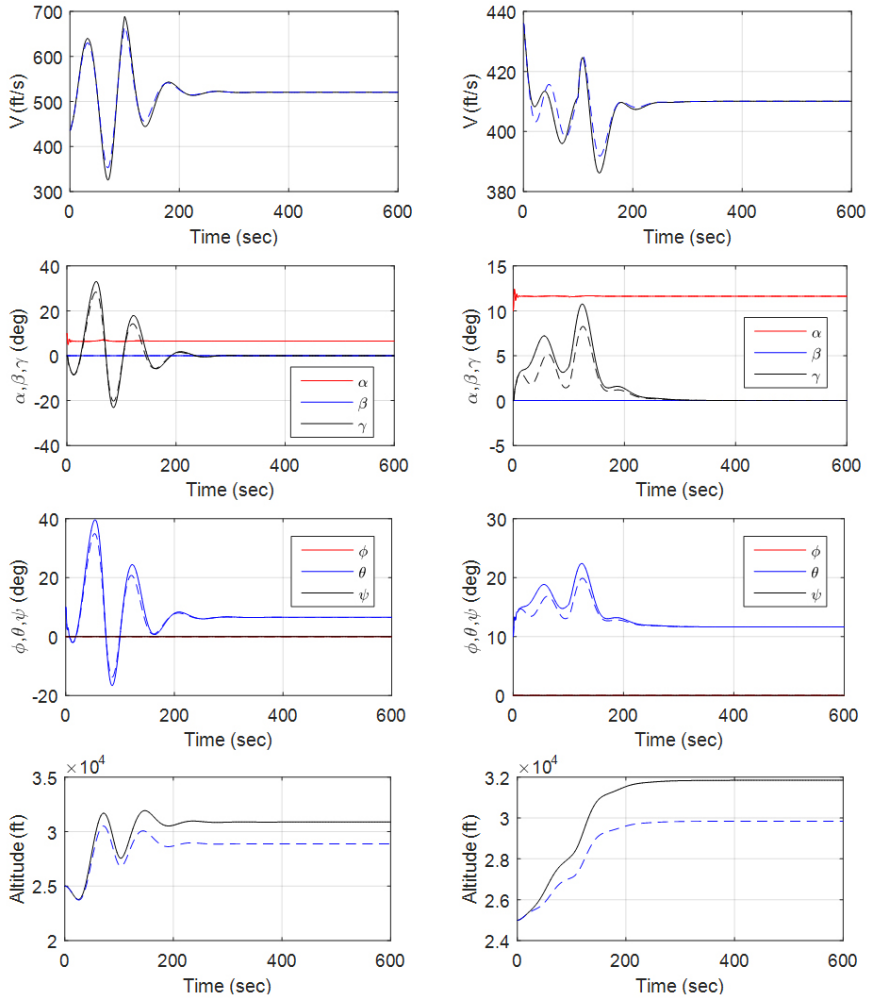

Figure 19. The response of the aircraft with reconfigured control to accommodate elevator jam failure. Left column: Elevator jammed at 1.28° position - 7000ft ascent (solid line) and 5000ft ascent (dashed line), Right column: Elevator jammed at -2.54° position - 7000ft ascent (solid line) and 5000ft ascent (dashed line).

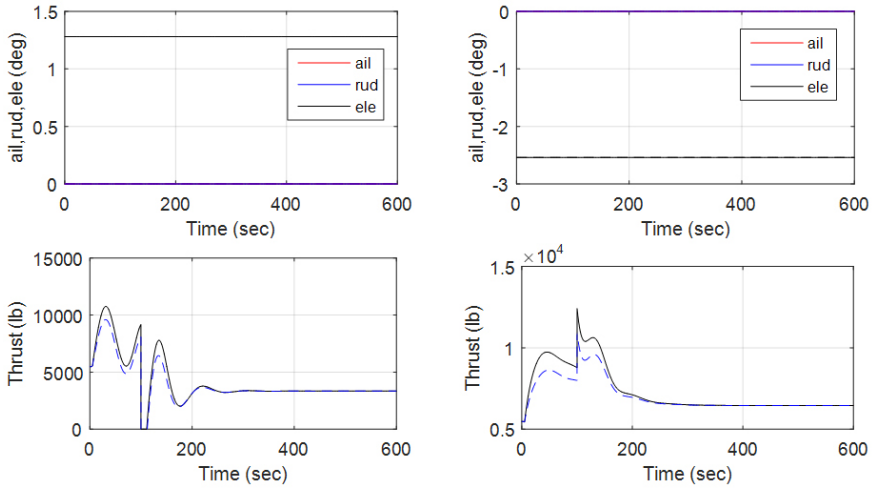

Figure 20. The control input of the aircraft with reconfigured control to accommodate elevator jam failure. Left column: Elevator jammed at 1.28° position - 7000ft ascent (solid line) and 5000ft ascent (dashed line), Right column: Elevator jammed at -2.54° position - 7000ft ascent (solid line) and 5000ft ascent (dashed line).

by solving the following equations,

$$\begin{aligned} A_{Lg}W_j + \begin{bmatrix} B_e & 0 \end{bmatrix} + B_j U_j = 0 \\ C_{1uj}W_j + \begin{bmatrix} 0 & D_{11uj} \end{bmatrix} = 0 \end{aligned} \tag{19}$$

with $C_{1uj} = \begin{bmatrix} 0 & 1 & 0 & -1 \end{bmatrix}$ and $D_{11uj} = 1$ chosen for flight path tracking.

The same fixed reconfigured controller designed above is employed in two simulations: one with elevator jammed at 1.28° position, and the other one jammed at −2.54°. Part of the state responses and the thrust control action are shown in Figure 19 and Figure 20, in which the left column is for the case with elevator jammed at 1.28° and the right column is for the other case with elevator jammed at −2.54°.

It can be seen that the same fixed reconfigured controller is able to accommodate the elevator jammed at different positions and achieve flight path tracking and altitude ascent or descent by using the single remaining thrust control. It is interesting to observe that both cases reach straight level flight equilibriums at steady state but with different angles of attack, different velocities, and different amount of thrust control.

For the case with elevator jammed at −2.54°, the aircraft reaches the following equilibrium, *Equil J*1:

$$Equil\ J1: \begin{cases} x_{J1} = \begin{bmatrix} 410\text{ft/s} & 0^\circ & 11.6^\circ & 0^\circ/s & 0^\circ/s & 0^\circ/s & 0^\circ & 11.6^\circ & *^\circ & *\text{ft} & *\text{ft} & *\text{ft} \end{bmatrix}^T \\ u_{J1} = \begin{bmatrix} 0^\circ & 0^\circ & -2.54^\circ & 6447.9\text{lb} \end{bmatrix} \end{cases} \tag{20}$$

For the case with elevator jammed at 1.28°, the aircraft reaches the following equilibrium, *Equil J*2:

$$Equil\ J2: \begin{cases} x_{J2} = \begin{bmatrix} 520\text{ft/s} & 0^\circ & 6.5^\circ & 0^\circ/s & 0^\circ/s & 0^\circ/s & 0^\circ & 6.5^\circ & *^\circ & *\text{ft} & *\text{ft} & *\text{ft} \end{bmatrix}^T \\ u_{J2} = \begin{bmatrix} 0^\circ & 0^\circ & 1.28^\circ & 3336.1\text{lb} \end{bmatrix} \end{cases} \tag{21}$$

V. Conclusion

In this study, we have demonstrated that a state-space linear feedback controller designed based on the modified LQR and multivariable regulator/servomechanism theory can be extremely effective in preventing aircraft from getting into an loss-of-control (LOC) situation. The same controller also exhibits impressive capability in rescuing aircraft from LOC back to a safe flight. We also demonstrated that the engagement of a recovery feedback control could deepen the LOC crisis if the controller is not properly designed, the engaging time is wrong, or the actuating resources are not adequate. The nonlinearity and time delay due to the actuator saturation and rate limit actually cause more issues than the nonlinearity of the aircraft flight dynamics. The actuator saturation can send the aircraft to an undesired equilibrium like the Equil X in Section IIIC that would lead to a crash. Another main contribution of the paper is the proposed reconfigured controller design to address the elevator jam issue. The designed single fixed regulator/controller is able to accommodate a range of elevator jam positions and achieve flight path tracking and altitude control. The amazing property of the regulator/controller is that it allows the closed-loop system to optimally choose a desired equilibrium to fly according to the elevator jam position and the flight path command.

Acknowledgments

The authors would like to thank Dr. Christine Belcastro from NASA Langley Research Center for many valuable discussions on aircraft flight safety and aircraft loss-of-control issues.

References

[1](2015, August) Statistical summary of commercial jet airplane accidents. Worldwide operations 1959 - 2014. statsum.pdf. Boeing Commercial Airplanes. Seattle, WA. [Online]. Available: http://www.boeing.com/news/techissues/pdf/statsum.pdf

[2]C. M. Belcastro and J. V. Foster, "Aircraft loss-of-control accident analysis," in *Proceedings of the 2010 AIAA Guidance, Navigation, and Control Conference*, Toronto, Canada, Aug. 2010.

[3]C. M. Belcastro, L. Groff, L. Newman, J. V. Foster, D. A. Crider, and D. H. Klyde, "Preliminary analysis of aircraft loss of control accidents: Worst case precursor combinations and temporal sequencing," in *Proceedings of the 2014 AIAA Guidance, Navigation, and Control Conference*, National Harbor, MAryland, Jan. 2014.

[4]J. E. Wilborn and J. V. Foster, "Defining commercial aircraft loss-of-control: a quantitative approach,," in *Proceedings of the 2004 AIAA Atmospheric Flight Mechanics Conference*, 2004.

[5]H. G. Kwatny, J.-E. T. Dongmo, B.-C. Chang, G. Bajpai, M. Yasar, and C. M. Belcastro, "Nonlinear analysis of aircraft loss of control," *AIAA Journal of Guidance, Control, and Dynamics*, vol. 36, no. 1, pp. 149–162, 2013.

[6]S. B. Buttrill, P. D. Arbuckle, and K. D. Hoffler, *Simulation model of a twin-tail, high performance airplane*, ser. NASA Technical Memorandum 107601. Hampton, Virginia: NASA Langley Research Center, 1992.

[7]A. Chakraborty, P. Seiler, and G. J. Balas, "Susceptibility of f/a-18 flight controllers to the falling-leaf mode: Linear analysis," *AIAA Journal of Guidance, Control, and Dynamics*, vol. 34, no. 1, pp. 57–72, 2011.

[8]——, "Susceptibility of f/a-18 flight controllers to the falling-leaf mode: Nonlinear analysis," *AIAA Journal of Guidance, Control, and Dynamics*, vol. 34, no. 1, pp. 73–85, 2011.

[9]M. V. Cook, *Flight Dynamics Principles.* Arnold in Great Britain, John Wiley & Sons Inc, 1997.

[10]J. Roskam, *Airplane Flight Dynamcs and Automatic Flight Controls, Part I.* Roskam Aviation and Engineering Corporation, 1979.

[11]T. Kailath, *Linear Systems.* Prentice-Hall, 1980.

[12]H. Kwakernaak and R. Sivan, *Linear Optimal Control Systems.* John Wiley & Sons, Inc., 1972.

[13]J. Huang, *Nonlinear Output Regulation: Theory and Applications.* Society for Industrial Mathematics, 2004, vol. 8.

[14]H. G. Kwatny and K. D. Young, "The variable structure servomechanism," *Systems and Control Letters*, vol. 1, pp. 184–191, 1981.

[15]B. Chang, G. Bajpai, and H. Kwatny, "A regulator design to address actuator failures," in *Proceedings of the 40th IEEE Conference on Decision and Control*, vol. 2. IEEE, 2001, pp. 1454–1459.